


[View Journal Online](#)  
[View Article Online](#)

# Green synthesis of gold nanoparticles using *Sambucus ebulus* fruit extract, characterization, and antileishmanial, antibacterial, antioxidant, and photocatalytic activities

 Mohammad Ali Ebrahimzadeh <sup>1</sup>, Seyedeh Roya Alizadeh <sup>1</sup> and Zahra Hashemi <sup>2,\*</sup>
<sup>1</sup> Department of Medicinal Chemistry, School of Pharmacy and Pharmaceutical Sciences Research Center, Mazandaran University of Medical Sciences, Sari, Mazandaran, Iran

<sup>2</sup> Department of Medicinal Chemistry, Faculty of Pharmacy, Ayatollah Amoli Branch, Islamic Azad University, Amol, Mazandaran, Iran

 \* Corresponding author at: Department of Medicinal Chemistry, Faculty of Pharmacy, Ayatollah Amoli Branch, Islamic Azad University, Amol, Mazandaran, Iran.  
 e-mail: [hngmhashemi@gmail.com](mailto:hngmhashemi@gmail.com) (Z. Hashemi).

## RESEARCH ARTICLE

## ABSTRACT



doi 10.5155/eurjchem.14.2.223-230.2403

Received: 24 December 2022

Received in revised form: 07 February 2023

Accepted: 01 March 2023

Published online: 30 June 2023

Printed: 30 June 2023

## KEYWORDS

*Sambucus ebulus* L.  
 Gold nanoparticles  
 Antioxidant activity  
 Antibacterial activity  
 Antileishmanial activity  
 Methyl orange degradation

In this study, gold nanoparticles were synthesized using the fruit extract of *Sambucus ebulus* (*S. ebulus*) as a reducing, capping, and stabilizing agent. Biogenic synthesis of gold nanoparticles (Au nanoparticles) was accomplished using *S. ebulus* fruit extract in the presence of hydrogen tetrachloroaurate(III) trihydrate at a temperature of 65 °C and the solution stirred at 400 rpm. The characterization of the synthesized nanoparticles (SE-AuNPs) was performed using different analytical methods, such as scanning electron microscopy (FE-SEM), energy dispersion X-ray spectroscopy (EDS), Fourier transform infrared (FT-IR), X-ray diffraction analysis (XRD), and UV-vis spectroscopy. A strong absorption peak at 565 nm confirmed the formation of the gold nanoparticle. On the basis of the electron microscopy results, AuNPs were mostly spherical with an average size of 116.2 nm. The cubic crystalline structure of the prepared nanoparticles was confirmed using the XRD pattern and the average crystallite size was obtained at 28.471 nm. FT-IR analysis confirmed the presence of functional groups in the plant extract for the synthesis of nanoparticles. SE-AuNPs showed good antibacterial activity against Gram-positive and Gram-negative bacteria tested and exhibited potent antileishmanial activity. Furthermore, SE-AuNPs showed excellent antioxidant activity that inhibited DPPH radicals with an IC<sub>50</sub> value of 21.976 µg/mL. The prepared AuNPs acted to degrade methyl orange (MO), which was performed in sodium borohydride and visible light.

 Cite this: *Eur. J. Chem.* 2023, 14(2), 223-230

 Journal website: [www.eurjchem.com](http://www.eurjchem.com)

## 1. Introduction

Nanoparticles have various applications such as catalysts, chemical sensors, electronic components, pharmaceutical products, medical diagnostic imaging, and antimicrobial effects [1-4]. Nanoparticle synthesis using the plant is simple and cost-effective [1]. Many studies show that biomolecules, such as proteins, phenols, and flavonoids, play an essential role in the reducing, capping, and stabilizing of nanoparticles [2]. Gold nanoparticles have many useful applications in biomedicine, catalysis, biosensing, electronic, and magnetic devices [3]. Gold nanoparticles have been used for different applications, such as antioxidants [4], anticancer drugs [5], antimicrobials [6], larvicides [7], agriculture [8], and drug delivery [9,10]. Green synthesis of gold nanoparticles using different plants such as *Panax ginseng* [11], *Chenopodium album* [12], *Avera lanata* [13], *Moringa oleifera* petals [14], *Sorbus aucuparia* [15], *Pleurotus ostreatus* [16], *Terminalia catappa* [17], *Mangifera indica* [18], *Anacardium occidentale* [19], *Murraya koenigii* [20], *Convolvulus fruticosus* and *Crataegus monogyna* [21] has been investigated. In the present research, *Sambucus ebulus* fruit extracts were employed as stabilizing and capping agents for

the biosynthesis of gold nanoparticles. The *S. ebulus* fruit has phenols and flavonoids that can act as reducing and capping agents for metal nanoparticle synthesis.

*S. ebulus*, or dwarf elder with white flowers, is located in Europe and West Asia [22]. Important phytochemicals of *S. ebulus* are steroids, flavones, tannic acids, glycoside compounds, ebulin, caffeic acid, cardiac glycosides, chlorogenic acid, and volatile compounds [23,24]. The existence of polyphenolic compounds can also be related to their antioxidant action [25]. *S. ebulus* exhibited different activities such as antioxidant and anti-inflammatory activities [26], biochemical effects, cytotoxic and antiangiogenic effects, antimicrobial and anticancer activities, improvement of the lipid profile, anti-parasitic, antiulcerogenic, and wound healing effects [24,27-29]. The antiemetic and neuroprotective activities of this plant have also been reported [30]. Iron (Fe<sup>2+</sup>) chelating ability of the methanolic extract of *S. ebulus* L. has been reported and has sent out free radicals to the outside of the body [31].

Leishmaniasis is a tropical disease that is created by the genus *Leishmania* parasites. The World Health Organization (WHO) has identified leishmaniasis as a category one disease [32]. Leishmaniasis has increased around the world, which has

been associated with a possible increase in disease vectors along with global warming [33]. The high toxicity and resistance to existing antileishmanial drugs [34] require further research to find effective and selective therapeutic agents. Medicinal plants screening for the synthesis of metal nanoparticles can be used to discover new, efficient, less toxic, and cost-effective antileishmanial agents [32].

AuNPs are inert and relatively resistant to bacteria and have unique optical, physical, and chemical properties with a rich history since ancient times and an intense future in the field of biological and chemical sciences. There is an increased requirement to develop eco-friendly methods to synthesize nanoparticles without applying toxic. The range of eco-friendly nanoparticle synthesis approaches includes the use of enzymes, microorganisms, plant extracts, and medicinal plants [35].

In the study, gold nanoparticles were prepared using *S. ebulus* fruit extracts and characterized by various analytical techniques such as UV/Vis spectroscopy, X-ray diffraction (XRD), energy dispersive X-ray spectroscopy (EDX), Fourier transform infrared (FT-IR) spectroscopy, and scanning electron microscopy (SEM). We demonstrated that the green synthesized nanoparticles displayed effective antileishmanial, antibacterial, and antioxidant activities and effectively eliminated the environment-polluting dye methyl orange.

## 2. Experimental

### 2.1. Chemicals

Hydrogen tetrachloroaurate(III) trihydrate ( $\text{HAuCl}_4 \cdot 3\text{H}_2\text{O}$ ), sodium borohydride, and 2,2-diphenyl-1-picrylhydrazyl (DPPH) were purchased from Sigma Aldrich (USA), Merck (Germany), and Fluka. Methyl orange and other chemicals were purchased from Merck India Ltd.

### 2.2. Preparation of the extract

The preparation of the *S. ebulus* fruit extract was carried out using the maceration method with methanol solvent. The *S. ebulus* fruit was dried at room temperature for three weeks and cut into small pieces. 100 g of small dried fruits with 250 mL of methanol were macerated for 24 hours. The filtration of the extract was carried out by Whatman filter paper (No. 1), then concentrated using a rotary evaporator, and then freeze-dried.

### 2.3. Biosynthesis of gold nanoparticles

10 mL of *S. ebulus* extract (0.1 mg/mL) was added to the freshly prepared  $\text{HAuCl}_4 \cdot 3\text{H}_2\text{O}$  solution (10 mL and 1 mM). The reaction mixture was heated to 65 °C with stirring until a change in color (reddish brown). Within 30 minutes, the reduction reaction was complete. In this case, the color change indicates that gold nanoparticles have formed ( $\text{Au}^{3+} \rightarrow \text{Au}^0$ ). A centrifuge (Centrifuge 5810R, Eppendorf, Germany) was used (6000 rpm and 20 min) to obtain gold nanoparticles. The precipitate obtained was washed with methanol and deionized water. The final product was placed in an oven to be analyzed and identified (60 °C).

### 2.4. Characterization

The green synthesized AuNPs were characterized by evaluating the absorbance of the mixture reaction on the UV-Vis spectrophotometer (T80 UV-Vis spectrophotometer, PGI, Beijing, China) at wavelengths between 200 and 800 nm. The functional groups of the *S. ebulus* L. fruit extract and the synthesized AuNPs were then evaluated using FT-IR analysis (ATR, Agilent, Cary 630, FTIR spectrometer, equipment at 4000 and 650  $\text{cm}^{-1}$ ). Solid forms of AuNPs were used for ATR-FTIR analysis without any manipulation. In ATR sampling, the IR

light travels through a crystal, which is internally reflected at least once at the crystal-sample interface; and the reflected light travels to the FTIR detector. During the internal reflection, a part of the IR light travels into the sample, where it can be absorbed.

XRD analysis was performed with monochromatic  $\text{CuK}\alpha$  radiation ( $\lambda = 1.54060 \text{ \AA}$ , step size =  $0.0195^\circ$ ) using a PANalytical X-PERT PRO diffractometer ( $2\theta = 10\text{-}80^\circ$ ) to determine the crystalline nature of AuNPs. Using Scherrer's formula,  $D = 0.9\lambda/\beta\cos\theta$  was obtained as the average crystallite size of the prepared AuNPs [9]. The field emission scanning electron microscope (FE-SEM) (TESCAN BRNO-Mira3 LMU) proved the surface homogeneity and uniformity of the NPs. Energy-dispersive X-ray analysis (EDX) along with FE-SEM confirmed the elemental composition analysis of the NPs.

### 2.5. Antibacterial test

MIC is known to be the lowest concentration of the antibacterial agent that inhibits the growth of a living organism. The MIC of synthesized SE-AuNPs was determined against *Enterococcus faecalis* (ATCC 29212) and *Staphylococcus aureus* (ATCC 29213) as Gram-positive bacteria, and *Escherichia coli* (ATCC 25922), *Proteus mirabilis* (ATCC 25933), *Acinetobacter baumannii* (ATCC 19606), *Pseudomonas aeruginosa* (ATCC 27853) and *Klebsiella pneumoniae* (ATCC 700603) as Gram-negative bacteria in 96-well microplate and using broth dilution methods. 100  $\mu\text{L}$  of Mueller Hinton broth (MHB) and various concentrations of SE-AuNPs were added to all wells in the 96-well microplate at ambient temperature. Then 100  $\mu\text{L}$  of dilute bacterial suspension (according to 0.5 McFarland turbidity standards) was added to a 96-well microplate. The plates were then incubated at 37 °C for 24 h. All solutions and synthesized nanoparticles were applied in a biosafety cabinet.

The MBC was introduced as the lowest concentration of the antibacterial agent that kills the organism entirely. The MBC test was performed by sub-culturing the suspension from each MIC well into the Muller-Hinton agar plate. Incubation was carried out for 24 h at 37 °C and the lowest concentration without bacterial growth on Muller-Hinton agar plates was determined as the MBC value. The reference compound was Ciprofloxacin.

### 2.6. DPPH radical scavenging assay

The antioxidant activity (*in vitro*) of SE-AuNPs was measured using the DPPH (diphenyl-1-picrylhydrazyl) assay method [29]. Concisely, 1 mL of different concentrations (41.25 to 2.6  $\mu\text{g}/\text{mL}$ ) of the synthesized AuNPs was mixed with 1 mL of DPPH (40 ppm) solution. Incubation was carried out in the dark at room temperature for 15 minutes. Then the absorbance of the reaction mixtures was determined at 517 nm by UV-vis spectroscopy. Butylated hydroxyanisole (BHA) was utilized as a positive control. The radical scavenging activity was calculated as a percentage inhibition using the following equation:

$$\text{Inhibition (\%)} = (A_c - A_s / A_c) \times 100 \quad (1)$$

where  $A_c$  and  $A_s$  are known as the absorbance of the control solution and the test sample. A linear regression analysis was carried out to determine the  $\text{IC}_{50}$  value of the samples.

### 2.7. Antileishmanial test

The Iranian strain of *L. major* promastigotes (MRHO/IR/75/ER) was cultured in RPMI-1640 medium (Gibco, Paisley, Scotland, UK) supplemented with 10% fetal bovine serum (FBS), 100  $\mu\text{g}/\text{mL}$  streptomycin, and 100 IU penicillin (Gibco, Paisley, Scotland, UK) at 24 °C.

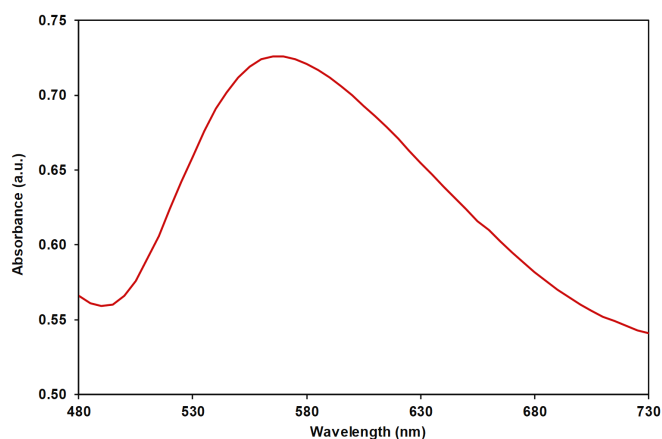


**Figure 1.** The UV-Vis spectra of biosynthesized gold nanoparticles displayed SPR peak at 565 nm; The mixture color of Auric chloride and plant fruit extract changes from light yellow to reddish-brown solution (SE-AuNPs).

The medium containing the parasite was sub-cultured every three days. Anti-amastigote activity was assessed using murine macrophage cell line J774A.1 prepared from the Iranian National Cell Bank (Pasteur Institute, Tehran, Iran) [36,37].

The anti-promastigote activity of SE-AuNPs was evaluated in 96-well plates for 72 hours. Serial dilutions of SS-AuNPs (12.5, 6.25, 3.12, and 1.56  $\mu\text{g}$ ) got ready in 100  $\mu\text{L}$  of RPMI-1640 medium and then, the addition of 100  $\mu\text{L}$  of RPMI-1640 medium (including  $1 \times 10^5$  promastigotes) was performed to each well. The negative control was three untreated wells comprising the parasite. After incubation of plates at 24  $^{\circ}\text{C}$  for 72 hours, a hemocytometer was used under a light microscope to calculate the number of promastigotes per milliliter (magnification  $\times 400$ ), which was accomplished by adding a solution of 2% formaldehyde (20  $\mu\text{L}$ ) in phosphate buffered saline at pH = 7.2. Positive control Amphotericin B and Glucantime that were investigated at concentrations of 0.00098-0.0078  $\mu\text{g}$  per 100  $\mu\text{L}$  of RPMI-1640 medium for Amphotericin B and 0.14-75  $\mu\text{g}$  per 100  $\mu\text{L}$  of RPMI-1640 medium for Glucantime. All examinations were done in triplicate. Equation (2) calculates the death rate (DR) of promastigotes:

$$\text{DR (\%)} = \frac{[\text{NC} - \text{DT}]}{\text{NC}} \times 100 \quad (2)$$

NC is the number of promastigotes in the negative control and DT is the number of promastigotes in each well treated [36,37].

The amount of  $2 \times 10^5$  cells of murine macrophage cells was added to each well in 200  $\mu\text{L}$  RPMI-1640 medium and its incubation was carried out (5%  $\text{CO}_2$ , 37  $^{\circ}\text{C}$ ). At the next stage, 200  $\mu\text{L}$  RPMI-1640 medium with the ratio of 1 cell: 10 promastigotes were poured into each well and incubated for 24 h. After incubation, well washing was performed with RPMI-1640 medium to remove excess parasites. Then, SE-AuNPs at various concentrations were added to each well and incubated for 72 h. Subsequently, excess fluid was removed and 50  $\mu\text{L}$  of MTT solution (5 mg/mL of stock solution in PBS) was added to each well (incubated for 4 h). After adding 100  $\mu\text{L}$  of DMSO, the optical absorbance was defined using a multi-scanning spectrophotometer (BioTek, Winooski, VT, USA) at 570 nm. Equation (3) estimated cell death rate:

$$\text{DR (\%)} = 1 - \frac{\text{AT}}{\text{AC}} \times 100 \quad (3)$$

The AT and AC are the mean absorbance of SE-AuNPs (each concentration) and the mean absorbances for the negative control, respectively. The selectivity index (SI) was measured by dividing  $\text{CC}_{50}$  by  $\text{IC}_{50}$  (amastigote) for SE-AuNPs. GraphPad

Prism (version 6) was used to determine  $\text{IC}_{50}$  and  $\text{CC}_{50}$  values [36,37].

## 2.8. Photocatalytic degradation of methyl orange (MO)

The photocatalytic effect of green synthesized SE-AuNP was assessed using the degradation of the organic dye of methyl orange (MO) in the presence of  $\text{NaBH}_4$ . 2 mL of deionized water was added to 50  $\mu\text{L}$  of 5 mM MO and 100  $\mu\text{L}$  of fresh 0.1 M  $\text{NaBH}_4$ . Then 30, 50, and 70  $\mu\text{L}$  of green synthesized AuNPs were added to the reaction mixture. The degradation process was checked by UV-vis spectra at different times. The kinetics of the reaction can be defined as in  $(A_t/A_0) = -kt$ , where k is the apparent first-order rate constant ( $\text{min}^{-1}$ ), t is the reaction time.  $A_t$  and  $A_0$  are known as the absorption of dyes at times t and 0, respectively [38].

## 3. Results and discussion

### 3.1. Characterization of green synthesized gold nanoparticles

The green method for the synthesis of metal nanoparticles is eco-friendly, inexpensive, safe, and rapid [39]. In the present study, the gold nanoparticles were prepared using the *Sambucus ebulus* fruit extract as the reducing and capping agent, which was confirmed by visible color change and absorption peaks in the UV-vis spectra. Au(III) ions were reduced to metallic nanoparticles and displayed a characteristic localized surface plasmon resonance (LSPR), where metal electrons in the conduction band collectively oscillate in resonance upon interaction with the light of a specific wavelength. Particle size, shape, and the reaction medium are effects on localized surface plasmon resonance. The absorption spectra of AuNP synthesized from the fruit of *S. ebulus* are shown in Figure 1b [32]. The mixture color of Auric chloride and plant fruit extract changes from light yellow to reddish-brown solution in 30 min and shows the SPR peak at 565 nm (Figure 1). The locations of the peak in the UV-visible spectrum are mainly influenced by the shape of the particles, the temperature, and the dielectric constant of the medium, indicating the dispersibility of the NPs, while the shape of the UV-visible peak defines the morphology of the NPs [40]. Broad and asymmetric SPR bands demonstrate that the prepared NPs are anisotropic and that the narrow band suggests the spherical shape of the nanoparticles.

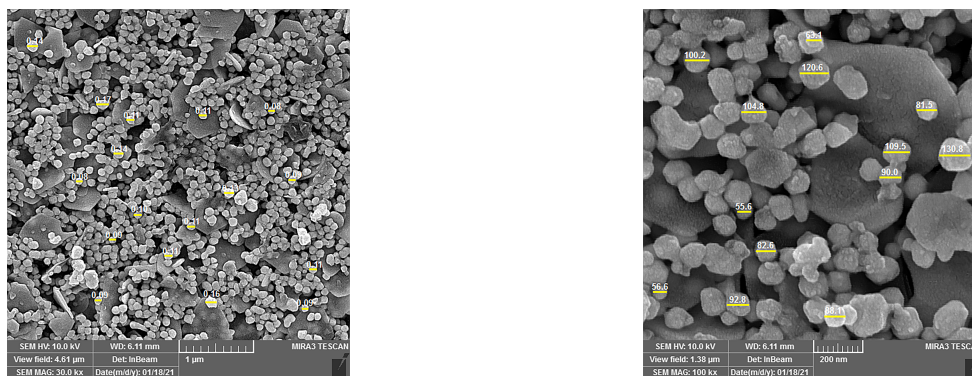


**Figure 2.** SEM images of SE-AuNPs at two scales 1 µm and 200 nm displayed spherical shapes with an average size of 116.2 nm.

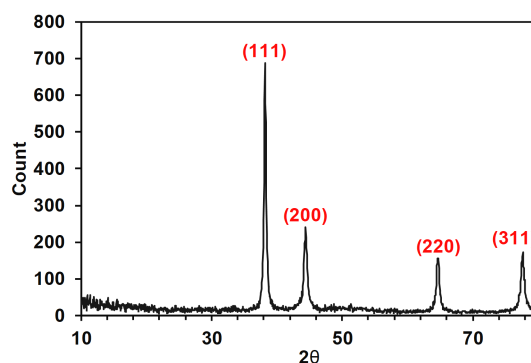


**Figure 3.** The XRD patterns of the synthesized AuNPs were observed at angles ( $2\theta$ ) of corresponding to (111), (200), (220), and (311) diffraction planes of the cubic structure of metallic Au.

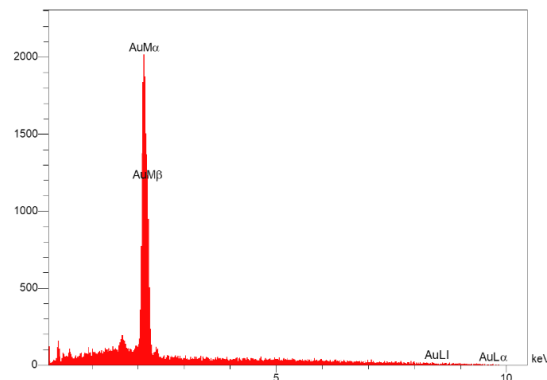


**Figure 4.** The EDX analysis of SE-AuNPs displayed a strong peak for Au.

The SEM image of SE-AuNPs displayed spherical shapes with an average size of 116.2 nm, as shown in Figure 2. The XRD pattern determined the crystalline nature and the average particle size of the biosynthesized AuNPs. The XRD patterns of the synthesized AuNPs were observed at angles ( $2\theta$ ) of 38.20, 44.40, 64.68, and 77.64° corresponded to the diffraction planes (111), (200), (220) and (311) of the cubic structure of metallic Au that Figure 3 confirmed the crystalline nature of the nanoparticles [9,41]. The planes of (200), (220), and (311) were smaller than those of (111), demonstrating that the prepared nanoparticles were extremely orientated in the plane (111) [41]. The mean size of the crystallite obtained from the XRD study was 28.741 nm. The EDX of SE-AuNPs exhibited a strong single for Au (Figure 4). To determine the functional groups of the *S. ebulus* fruit extract, FTIR spectroscopy was used, which is responsible for the reduction and stabilization of synthesized AuNPs. The FTIR spectrum of extracts (Figure 5) demonstrated

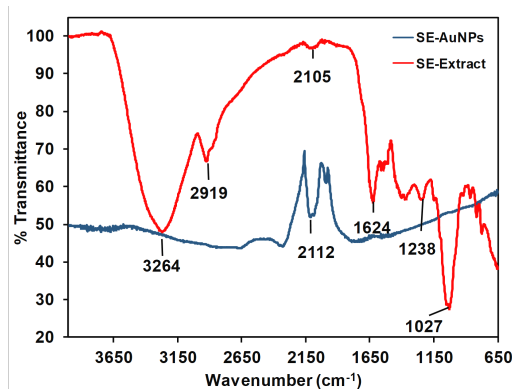
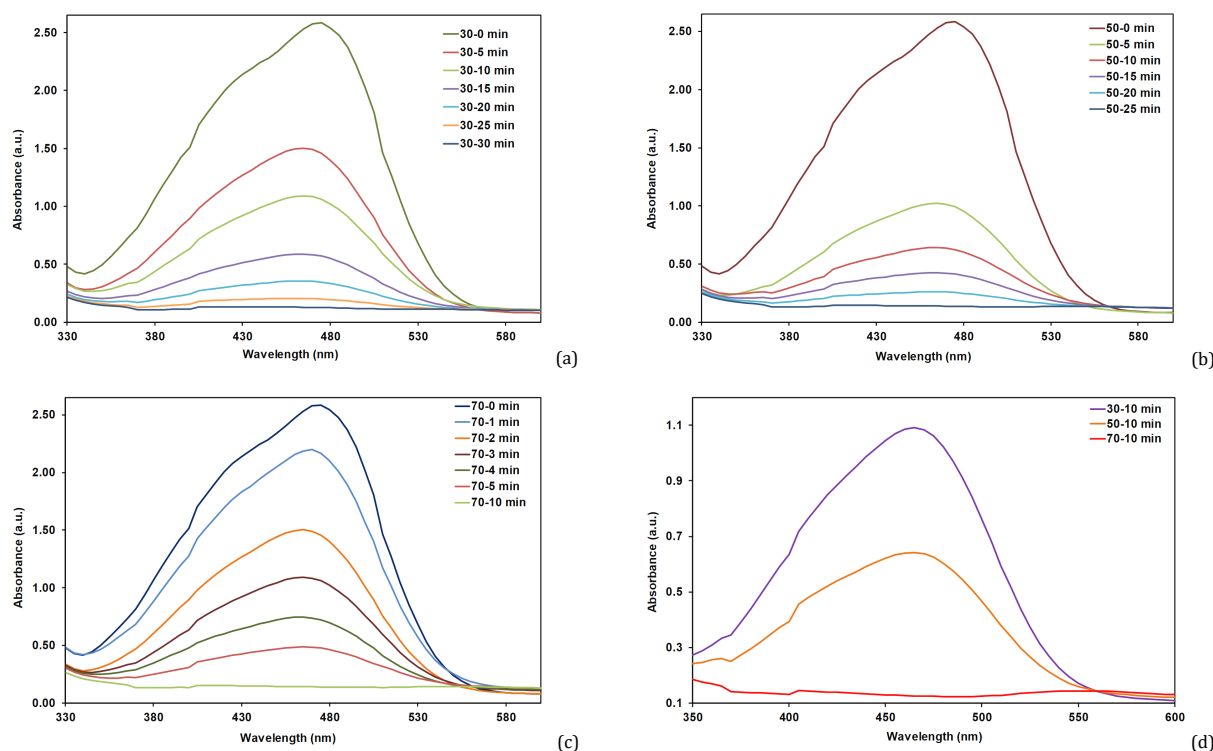
peaks at 3264  $\text{cm}^{-1}$  related to O-H stretch, H-bonded phenols/alcohols, at 2919  $\text{cm}^{-1}$  corresponded to C-H stretching, 2105  $\text{cm}^{-1}$  for  $\text{-C}\equiv\text{C-}$  stretching, 1624  $\text{cm}^{-1}$  for  $\text{-C=C-}$  stretching, 1238  $\text{cm}^{-1}$  for C-O stretching, 1027  $\text{cm}^{-1}$  for C-N stretching of aliphatic amines [42-44]. This data confirmed the key role of different phytochemicals in the synthesizing and stabilizing of metal nanoparticles. Changing the intensity or shift in the NPs spectra was related to the phytochemicals' coordination with the surface of the metal.

### 3.2. Antibacterial activities

Small AuNPs can penetrate bacteria and cause damage, decrease their activity, and lead to cell death [45]. In this study, the antimicrobial activity of the prepared AuNPs was investigated against several bacteria by determining the MIC.

**Table 1.** Antibacterial activity of green-synthesized AuNPs on ATCC strains.

Bacteria	ATCC	SE-AuNPs	
		MIC ( $\mu\text{g/mL}$ )	MBC ( $\mu\text{g/mL}$ )
<i>S. aureus</i>	ATCC 29213	20.625	660
<i>E. faecalis</i>	ATCC 29212	41.25	660
<i>P. aeruginosa</i>	ATCC 27853	41.25	1320
<i>A. baumannii</i>	ATCC 19606	41.25	1320
<i>E. coli</i>	ATCC 25922	41.25	660
<i>K. pneumoniae</i>	ATCC 700603	41.25	1320
<i>P. mirabilis</i>	ATCC 25933	20.625	660

**Figure 5.** FTIR spectra of the extracts displaying functional groups confirmed the key role of different phytochemicals in the synthesis and stabilization of metal nanoparticles.**Figure 6.** The UV-Vis absorbance spectra of MO mixed with  $\text{NaBH}_4$  solution in the presence of different volumes of SS-AuNPs as catalyst: a) 30  $\mu\text{L}$  of SS-AuNPs; b) 50  $\mu\text{L}$  of SS-AuNPs; c) 70  $\mu\text{L}$  of SS-AuNPs at time intervals. d) Comparison of the colorization of power in different volumes (30, 50, and 70  $\mu\text{L}$ ) of SE-AuNPs at a specified time.

The MIC and MBC obtained from this investigation are presented in Table 1. According to the data, the lowest MIC of the synthesized AuNPs, 20.625  $\mu\text{g/mL}$ , was observed for *S. aureus* and *P. mirabilis*, and the MBC was obtained 660  $\mu\text{g/mL}$  for these two bacteria. The SE-AuNPs inhibited *S. aureus* and *P. mirabilis* more than other bacteria. The reference antibiotic

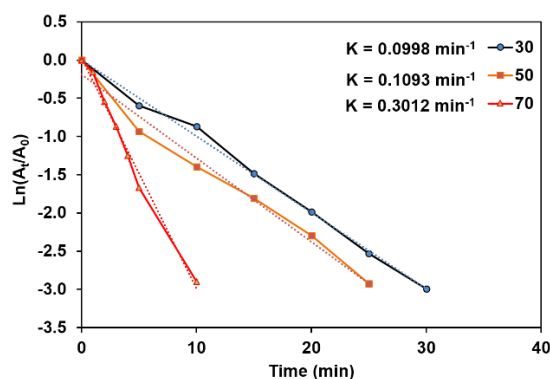
ciprofloxacin exhibited MIC values of 0.21 and 0.25  $\mu\text{g/mL}$  for *S. aureus* and *P. mirabilis*.

### 3.3. DPPH free radical scavenging assay

The antioxidant reducing capacity of various compounds is directly related to antioxidant activity [42,46].

**Table 2.** Antileishmanial activity of metal nanoparticles prepared by green synthesized methods.

Plant mediated various Nanoparticles	Concentration of Drug-treated promastigotes ( $\mu\text{g/L}$ )	IC <sub>50</sub> promastigotes ( $\mu\text{g/L}$ )	Concentration of Drug-treated amastigotes ( $\mu\text{g/L}$ )	IC <sub>50</sub> amastigotes ( $\mu\text{g/L}$ )	Reference
<i>Sambucus ebulus</i> -AuNPs	12.5-1.56	4.75	12.5-1.56	4.4	Present work
<i>Allium paradoxum</i> -SeNPs	0.17-175	35.49	-	-	[55]
<i>Cannabis sativa</i> -AuNPs	-	-	1000-50	171	[56]
<i>Berberis vulgaris</i> -AgNPs	25-3.12	10.88	25-3.12	8.29	[57]
<i>Scrophularia striata</i> -AgNPs	9.37-1.17	4.03	9.37-1.17	2.49	[58]
<i>Ferula persica</i> -AgNPs	78.12-9.76	23.14	78.12-9.76	26.43	[52]
<i>Crocus caspius</i> -AuNPs	212.5-6.64	13.92	-	-	[59]
<i>Alsea rosea</i> -AgNPs	7.8-0.97	2.2	7.81-0.97	4.13	[60]
Glucantime	75-0.14	19.95	75-0.14	33.09	-

**Figure 7.** The degradation rate of MO in three concentrations was 30, 50, and 70  $\mu\text{L}$  of SE-AuNPs.

The damage created by free radicals in various major diseases can be protected by antioxidants [47]. Various studies have introduced green synthesized gold nanoparticles as strong antioxidants [2,44,48,49]. The ability of nanoparticles (SE-AuNPs) to reduce DPPH was evaluated by observing a color change, and the control showed no color change. SE-AuNPs at concentrations 41.25 to 6.58  $\mu\text{g/mL}$  were evaluated using the DPPH scavenging assay at an absorbance at 517 nm. As a positive control, BHA exhibited an IC<sub>50</sub> value of 53.96  $\mu\text{g/mL}$ . The DPPH scavenging activity of SE-AuNPs increased dose-dependently. By adding the DPPH solution in the synthesized gold nanoparticles, the color of the solution changed, and the responsibility for the absorbance at 517 nm may be due to the scavenging of DPPH by donating an electron or the hydrogen atom to the stable DPPH structure. The results of the DPPH assay indicated that SE-AuNPs exhibited effective free radical inhibition with an IC<sub>50</sub> value of 22.15 $\pm$ 0.37  $\mu\text{g/mL}$ . Thus, SE-AuNPs were more effective than BHA in inhibiting free radicals.

### 3.4. Anti-leishmanial activities

Leishmaniasis is one of the deadliest diseases worldwide, and antileishmaniasis treatments are related to several drawbacks. Therefore, the development of new antileishmanial strategies is needed [32]. Metal nanoparticles produce reactive oxygen species (ROS) such that Leishmania is very sensitive to ROS, and the drug that can produce ROS will be an effective antileishmaniasis agent. Macrophages generate a high concentration of ROS to destroy microbial agents [50,51]. However, Leishmania bypasses ROS oxidative damage by inhibiting enzymes involved in the ROS production process [32]. In this study, the IC<sub>50</sub> value for the anti-promastigotes activity of SE-AuNPs was measured to be 4.75  $\mu\text{g}$ . Therefore, a statistically significant difference was observed between the IC<sub>50</sub> values of SE-AuNPs and amphotericin B (IC<sub>50</sub> = 0.0016,  $p < 0.0001$ ) and glucantime (IC<sub>50</sub> = 0.0016,  $p < 0.0001$ ). The IC<sub>50</sub> value for the anti-amastigote activity of SE-AuNPs was calculated to be 4.4  $\mu\text{g}$  that was 0.0011 and 33.09 for Amphotericin B and Glucantime, respectively. A significant difference was observed between the IC<sub>50</sub> values of SE-AuNPs and positive controls of amphotericin B

( $p < 0.0001$ ) and glucantime ( $p < 0.0001$ ). SI values were obtained at 5.5, 19.4, and 16.33 for SE-AuNPs, amphotericin B and glucantime. There have been several studies reporting the antileishmanial activity of biosynthesized nanoparticles (Table 2). Leishmania parasites produce ROS through modulation of a signaling cascade moiety. The intracellular ROS formed by macrophages drives the oxidation of NPs, which further enhances ROS production. Therefore, it can be hypothesized that SE-AuNPs could activate macrophages for ROS production and inhibit amastigote growth significantly without inducing death in the macrophage population together with the ROS, phytochemicals (capping and stabilizing agents) released from SE-AuNPs may enhance antileishmanial activity by safeguarding the host cells [52].

### 3.5. Photo-catalytic activity of AuNPs

The catalytic activity of synthesized AuNPs was studied on the degradation of methyl orange (MO) using NaBH<sub>4</sub>. In the absence of a nanocatalyst, the reducing power of NaBH<sub>4</sub> is very low [53]. According to Figure 6, when NaBH<sub>4</sub> solution was added to MO, the absorption intensity of MO decreased very slowly at wavelength 470 nm. Interestingly, MO degradation was performed by adding different volumes of synthesized AuNPs to a mixture of MO and NaBH<sub>4</sub> solution. Figure 6 confirmed that MO azo dye with orange color reduced to colorless hydrazine derivatives [54]. Volumes 30, 50, and 70  $\mu\text{L}$  of prepared AuNPs, completely degraded MO in 30, 30, and 10 min, respectively (Figure 6). UV-vis spectra monitored the rate of dye degradation. The maximum intensity obtained from the degradation reaction gradually decreased at 470 nm, and the rate constants were determined as 0.0998, 0.1093, and 0.3012 min<sup>-1</sup>, respectively (Figure 7). On the basis of the gained data, the rate constant enhanced with increasing the concentration of green synthesized AuNPs. The surface area of the active site of nanoparticles increased with increasing concentration of gold nanoparticles. Therefore, the biosynthesized AuNPs had a potential photocatalytic effect on the degradation of the MO azo dye.

#### 4. Conclusions

Biosynthesizing AuNPs was successfully performed by a simple, safe, stable, and eco-friendly method using fruit extracts of *S. ebulus* L. In the synthesis of AuNPs, *S. ebulus* L. extract acted as reducing as well as capping agents, and FTIR studies confirmed the presence of effective phytochemicals. The microscopic data demonstrated that AuNPs mainly were spherical, with an average particle size of 116.2 nm. XRD pattern confirmed the cubic crystalline structure of the prepared AuNPs, and the average crystallite size was calculated as 28.471 nm. Synthesized SE-AuNPs displayed an excellent antibacterial effect against tested bacteria (*Pseudomonas aeruginosa*, *Proteus mirabilis*, *Klebsiella pneumonia*, *Staphylococcus aureus*, *Enterococcus faecalis*, *Acinetobacter baumannii*, and *Escherichia coli*), especially against *S. aureus* and *P. mirabilis* with MIC value of 20.625 µg/mL. Besides, SE-AuNPs indicated strong antileishmanial activity and great DPPH inhibition activity (IC<sub>50</sub> = 15.81 µg/mL). Besides, the synthesized AuNPs eliminated methyl orange (MO) in the presence of sodium borohydride and visible light.

#### Acknowledgements

Research reported in this publication was supported by the Elite Researcher Grant Committee under the award number [958433] from the National Institute for Medical Research Development (NIMAD), Tehran, Iran.

#### Disclosure statement


Conflict of interest: The authors declare that they have no conflict of interest. Ethical approval: All ethical guidelines have been adhered to. Sample availability: Samples of the compounds are available from the author.

#### CRedit authorship contribution statement

Conceptualization: Mohammad Ali Ebrahimzadeh; Methodology: Mohammad Ali Ebrahimzadeh, Seyedeh Roya Alizadeh; Formal analysis: Mohammad Ali Ebrahimzadeh, Seyedeh Roya Alizadeh; Investigation: Mohammad Ali Ebrahimzadeh, Seyedeh Roya Alizadeh; Resources: Zahra Hashemi; Funding: Zahra Hashemi; Supervision: Zahra Hashemi; Writing - Original Draft: Mohammad Ali Ebrahimzadeh, Seyedeh Roya Alizadeh, Zahra Hashemi; Review and Editing: Zahra Hashemi.


#### ORCID and Email


Mohammad Ali Ebrahimzadeh

 [zadeh20@gmail.com](mailto:zadeh20@gmail.com)

 <https://orcid.org/0000-0002-8769-9912>

Seyedeh Roya Alizadeh

 [r.alizadeh.2019@gmail.com](mailto:r.alizadeh.2019@gmail.com)

 <https://orcid.org/0000-0001-7435-4635>

Zahra Hashemi

 [hngmhashemi@gmail.com](mailto:hngmhashemi@gmail.com)

 <https://orcid.org/0000-0002-6889-1976>

#### References

- Gan, P. P.; Ng, S. H.; Huang, Y.; Li, S. F. Y. Green synthesis of gold nanoparticles using palm oil mill effluent (POME): a low-cost and eco-friendly viable approach. *Bioresour. Technol.* **2012**, *113*, 132–135.
- Sathishkumar; Jha, P. K.; Vignesh; Rajkuberan; Jeyaraj; Selvakumar; Jha, R.; Sivaramakrishnan Cannonball fruit (*Couroupita guianensis*, Aubl.) extract mediated synthesis of gold nanoparticles and evaluation of its antioxidant activity. *J. Mol. Liq.* **2016**, *215*, 229–236.
- Lukman, A. I.; Gong, B.; Marjo, C. E.; Roessner, U.; Harris, A. T. Facile synthesis, stabilization, and anti-bacterial performance of discrete Ag nanoparticles using *Medicago sativa* seed exudates. *J. Colloid Interface Sci.* **2011**, *353*, 433–444.
- Sengani, M.; Rajeswari, D. Identification of potential antioxidant indices by biogenic gold nanoparticles in hyperglycemic Wistar rats. *Environ. Toxicol. Pharmacol.* **2017**, *50*, 11–19.
- Rajeshkumar, S. Anticancer activity of eco-friendly gold nanoparticles against lung and liver cancer cells. *J. Genet. Eng. Biotechnol.* **2016**, *14*, 195–202.
- Dorosti, N.; Jamshidi, F. Plant-mediated gold nanoparticles by *Dracocephalum kotschy* as anticholinesterase agent: Synthesis, characterization, and evaluation of anticancer and antibacterial activity. *J. Appl. Biomed.* **2016**, *14*, 235–245.
- Balasubramani, G.; Ramkumar, R.; Krishnaveni, N.; Sowmiya, R.; Deepak, P.; Arul, D.; Perumal, P. GC-MS analysis of bioactive components and synthesis of gold nanoparticle using *Chloroxylon swietenia* DC leaf extract and its larvicidal activity. *J. Photochem. Photobiol. B* **2015**, *148*, 1–8.
- Mahakham, W.; Theerakulpisut, P.; Maensiri, S.; Phumying, S.; Sarmah, A. K. Environmentally benign synthesis of phytochemicals-capped gold nanoparticles as nanopriming agent for promoting maize seed germination. *Sci. Total Environ.* **2016**, *573*, 1089–1102.
- Balalakshmi, C.; Gopinath, K.; Govindarajan, M.; Lokesh, R.; Arumugam, A.; Alharbi, N. S.; Kadaikunnan, S.; Khaled, J. M.; Benelli, G. Green synthesis of gold nanoparticles using a cheap *Sphaeranthus indicus* extract: Impact on plant cells and the aquatic crustacean *Artemia nauplii*. *J. Photochem. Photobiol. B* **2017**, *173*, 598–605.
- Ghorbani, M.; Hamishehkar, H. Redox and pH-responsive gold nanoparticles as a new platform for simultaneous triple anti-cancer drugs targeting. *Int. J. Pharm.* **2017**, *520*, 126–138.
- Singh, P.; Kim, Y. J.; Yang, D. C. A strategic approach for rapid synthesis of gold and silver nanoparticles by *Panax ginseng* leaves. *Artif. Cells Nanomed. Biotechnol.* **2016**, *44*, 1949–1957.
- Dwivedi, A. D.; Gopal, K. Biosynthesis of silver and gold nanoparticles using *Chenopodium album* leaf extract. *Colloids Surf. A Physicochem. Eng. Asp.* **2010**, *369*, 27–33.
- Joseph, S.; Mathew, B. Microwave assisted facile green synthesis of silver and gold nanocatalysts using the leaf extract of *Aerva lanata*. *Spectrochim. Acta A Mol. Biomol. Spectrosc.* **2015**, *136*, 1371–1379.
- Anand, K.; Gengan, R. M.; Phulokdaree, A.; Chuturgoon, A. Agroforestry waste *Moringa oleifera* petals mediated green synthesis of gold nanoparticles and their anti-cancer and catalytic activity. *J. Ind. Eng. Chem.* **2015**, *21*, 1105–1111.
- Dubey, S. P.; Lahtinen, M.; Särkkä, H.; Sillanpää, M. Bioprospective of *Sorbus aucuparia* leaf extract in development of silver and gold nanocolloids. *Colloids Surf. B Biointerfaces* **2010**, *80*, 26–33.
- El-Batal, A. I.; ElKenawy, N. M.; Yassin, A. S.; Amin, M. A. Laccase production by *Pleurotus ostreatus* and its application in synthesis of gold nanoparticles. *Biotechnol. Rep. (Amst.)* **2015**, *5*, 31–39.
- Ankamwar, B. Biosynthesis of Gold Nanoparticles (Green-gold) Using Leaf Extract of *Terminalia Catappa*. *E-J. Chem.* **2010**, *7*, 1334–1339.
- Philip, D. Rapid green synthesis of spherical gold nanoparticles using *Mangifera indica* leaf. *Spectrochim. Acta A Mol. Biomol. Spectrosc.* **2010**, *77*, 807–810.
- Sheny, D. S.; Mathew, J.; Philip, D. Phytosynthesis of Au, Ag and Au-Ag bimetallic nanoparticles using aqueous extract and dried leaf of *Anacardium occidentale*. *Spectrochim. Acta A Mol. Biomol. Spectrosc.* **2011**, *79*, 254–262.
- Philip, D.; Unni, C.; Aromal, S. A.; Vidhu, V. K. Murraya Koenigii leaf-assisted rapid green synthesis of silver and gold nanoparticles. *Spectrochim. Acta A Mol. Biomol. Spectrosc.* **2011**, *78*, 899–904.
- Shirzadi-Ahodashi, M.; Mortazavi-Derazkola, S.; Ebrahimzadeh, M. A. Biosynthesis of noble metal nanoparticles using *Crataegus monogyna* leaf extract (CML@X-NPs, X= Ag, Au): Antibacterial and cytotoxic activities against breast and gastric cancer cell lines. *Surf. Interfaces* **2020**, *21*, 100697.
- Kaya, Y.; Haji, E. K.; Arvas, Y. E.; Aksoy, H. M. *Sambucus ebulus* L.: Past, present and future. In *Proceedings of the 2nd International Conference on Biosciences and Medical Engineering (ICBME2019): Towards innovative research and cross-disciplinary collaborations*; AIP Publishing, 2019. <https://doi.org/10.1063/1.5125534>
- Ebrahimzadeh, M. A.; Mahmoudi, M.; Saiednia, S.; Pourmorad, F.; Salimi, E. Anti-inflammatory and anti-nociceptive properties of fractionated extracts in different parts of *Sambucus ebulus*. *J. Mazandaran Univ. Med. Sci.* **2006**, *16*, 35–47. <http://jmums.mazums.ac.ir/article-1-132-en.html>
- Ebrahimzadeh, M. A.; Mahmoudi, M.; Karami, M.; Saeedi, S.; Ahmadi, A. H.; Salimi, E. Separation of active and toxic portions in *Sambucus ebulus*. *Pak. J. Biol. Sci.* **2007**, *10*, 4171–4173.
- Jiménez, P.; Tejero, J.; Cordoba-Diaz, D.; Quinto, E. J.; Garrosa, M.; Gayoso, M. J.; Girbés, T. Ebulin from dwarf elder (*Sambucus ebulus* L.): a mini-review. *Toxins (Basel)* **2015**, *7*, 648–658.
- Barak, T. H.; Celep, E.; Inan, Y.; Yeşilada, E. In vitro human digestion simulation of the bioavailability and antioxidant activity of phenolics from *Sambucus ebulus* L. fruit extracts. *Food Biosci.* **2020**, *37*, 100711.
- Tasinov, O.; Kiselova-Kaneva, Y.; Ivanova, D. *Sambucus ebulus* - from traditional medicine to recent studies. *Scr. Sci. Medica* **2013**, *45*, 36–42.
- Saravi, S. S. S.; Shokrzadeh, M.; Hosseini Shirazi, F. Cytotoxicity of *Sambucus ebulus* on cancer cell lines and protective effects of vitamins C and E against its cytotoxicity on normal cell lines. *Afr. J. Biotechnol.* **2013**, *12*(21), 3360–3365.

- [29]. Shokrzadeh, M.; Saravi, S. S. S. The chemistry, pharmacology and clinical properties of *Sambucus ebulus*: A review. *J. Med. Plant Res.* **2010**, *4*, 095–103.
- [30]. Fathi, H.; Ebrahimzadeh, M. A.; Ziar, A.; Mohammadi, H. Oxidative damage induced by retching; antiemetic and neuroprotective role of *Sambucus ebulus* L. *Cell Biol. Toxicol.* **2015**, *31*, 231–239.
- [31]. Ebrahimzadeh, M. A.; Nabavi, S. F.; Nabavi, S. M. Antioxidant activities of methanol extract of *Sambucus ebulus* L. flower. *Pak. J. Biol. Sci.* **2009**, *12*, 447–450.
- [32]. Ahmad, A.; Syed, F.; Shah, A.; Khan, Z.; Tahir, K.; Khan, A. U.; Yuan, Q. Silver and gold nanoparticles from *Sargentodoxa cuneata*: synthesis, characterization and antileishmanial activity. *RSC Adv.* **2015**, *5*, 73793–73806.
- [33]. Peterson, A. T.; Shaw, J. *Lutzomyia* vectors for cutaneous leishmaniasis in Southern Brazil: ecological niche models, predicted geographic distributions, and climate change effects. *Int. J. Parasitol.* **2003**, *33*, 919–931.
- [34]. Natera, S.; Machuca, C.; Padrón-Nieves, M.; Romero, A.; Díaz, E.; Pontes-Sucre, A. *Leishmania* spp.: proficiency of drug-resistant parasites. *Int. J. Antimicrob. Agents* **2007**, *29*, 637–642.
- [35]. Al-Radadi, N. S. Facile one-step green synthesis of gold nanoparticles (AuNP) using licorice root extract: Antimicrobial and anticancer study against HepG2 cell line. *Arab. J. Chem.* **2021**, *14*, 102956.
- [36]. Akhtari, J.; Faridnia, R.; Kalani, H.; Bastani, R.; Fakhar, M.; Rezvan, H.; Beydokhti, A. K. Potent in vitro antileishmanial activity of a nanoformulation of cisplatin with carbon nanotubes against *Leishmania major*. *J. Glob. Antimicrob. Resist.* **2019**, *16*, 11–16.
- [37]. Faridnia, R.; Kalani, H.; Fakhar, M.; Akhtari, J. Investigating in vitro anti-leishmanial effects of silibinin and silymarin on *Leishmania major*. *Ann. Parasitol.* **2018**, *64*, 29–35.
- [38]. Akilandaaswari, B.; Muthu, K. Green method for synthesis and characterization of gold nanoparticles using *Lawsonia inermis* seed extract and their photocatalytic activity. *Mater. Lett.* **2020**, *277*, 128344.
- [39]. Rajan, A.; Rajan, A. R.; Philip, D. *Elettaria cardamomum* seed mediated rapid synthesis of gold nanoparticles and its biological activities. *OpenNano* **2017**, *2*, 1–8.
- [40]. Dhand, V.; Soumya, L.; Bharadwaj, S.; Chakra, S.; Bhatt, D.; Sreedhar, B. Green synthesis of silver nanoparticles using *Coffea arabica* seed extract and its antibacterial activity. *Mater. Sci. Eng. C Mater. Biol. Appl.* **2016**, *58*, 36–43.
- [41]. Vijaya Kumar, P.; Mary Jelastin Kala, S.; Prakash, K. S. Green synthesis of gold nanoparticles using *Croton Caudatus* Geisel leaf extract and their biological studies. *Mater. Lett.* **2019**, *236*, 19–22.
- [42]. Hashemi, Z.; Ebrahimzadeh, M. A.; Biparva, P.; Mortazavi-Derazkola, S.; Goli, H. R.; Sadeghian, F.; Kardan, M.; Rafiei, A. Biogenic silver and zero-valent iron nanoparticles by *Feijoa*: Biosynthesis, characterization, cytotoxic, antibacterial and antioxidant activities. *Anticancer Agents Med. Chem.* **2020**, *20*, 1673–1687.
- [43]. Geetha, R.; Ashokkumar, T.; Tamilselvan, S.; Govindaraju, K.; Sadiq, M.; Singaravelu, G. Green synthesis of gold nanoparticles and their anticancer activity. *Cancer Nanotechnol.* **2013**, *4*, 91–98.
- [44]. Naraginti, S.; Li, Y. Preliminary investigation of catalytic, antioxidant, anticancer and bactericidal activity of green synthesized silver and gold nanoparticles using *Actinidia deliciosa*. *J. Photochem. Photobiol. B* **2017**, *170*, 225–234.
- [45]. Bindhu, M. R.; Umadevi, M. Antibacterial activities of green synthesized gold nanoparticles. *Mater. Lett.* **2014**, *120*, 122–125.
- [46]. Zhao, H.; Dong, J.; Lu, J.; Chen, J.; Li, Y.; Shan, L.; Lin, Y.; Fan, W.; Gu, G. Effects of extraction solvent mixtures on antioxidant activity evaluation and their extraction capacity and selectivity for free phenolic compounds in barley (*Hordeum vulgare* L.). *J. Agric. Food Chem.* **2006**, *54*, 7277–7286.
- [47]. Hua, D.; Zhang, D.; Huang, B.; Yi, P.; Yan, C. Structural characterization and DPPH· radical scavenging activity of a polysaccharide from *Guara* fruits. *Carbohydr. Polym.* **2014**, *103*, 143–147.
- [48]. Shabestarian, H.; Homayouni-Tabrizi, M.; Soltani, M.; Namvar, F.; Azizi, S.; Mohamad, R.; Shabestarian, H. Green synthesis of gold nanoparticles using sumac aqueous extract and their antioxidant activity. *Mater. Res.* **2016**, *20*, 264–270.
- [49]. Pu, S.; Li, J.; Sun, L.; Zhong, L.; Ma, Q. An in vitro comparison of the antioxidant activities of chitosan and green synthesized gold nanoparticles. *Carbohydr. Polym.* **2019**, *211*, 161–172.
- [50]. Lodge, R.; Descoteaux, A. Phagocytosis of *Leishmania donovani* amastigotes is Rac1 dependent and occurs in the absence of NADPH oxidase activation. *Eur. J. Immunol.* **2006**, *36*, 2735–2744.
- [51]. Allahverdiyev, A. M.; Abamor, E. S.; Bagirova, M.; Ustundag, C. B.; Kaya, C.; Kaya, F.; Rafailovich, M. Antileishmanial effect of silver nanoparticles and their enhanced antiparasitic activity under ultraviolet light. *Int. J. Nanomedicine* **2011**, *6*, 2705–2714.
- [52]. Hashemi, Z.; Mohammadyan, M.; Naderi, S.; Fakhar, M.; Biparva, P.; Akhtari, J.; Ebrahimzadeh, M. A. Green synthesis of silver nanoparticles using *Ferula persica* extract (Fp-NPs): Characterization, antibacterial, antileishmanial, and in vitro anticancer activities. *Mater. Today Commun.* **2021**, *27*, 102264.
- [53]. Cyril, N.; George, J. B.; Nair, P. V.; Joseph, L.; Sunila; Smitha; Anila; Syllas. Catalytic activity of *Derris trifoliata* stabilized gold and silver nanoparticles in the reduction of isomers of nitrophenol and azo violet. *Nano-struct. Nano-Objects* **2020**, *22*, 100430.
- [54]. Jayapriya, M.; Dhanasekaran, D.; Arulmozhi, M.; Nandhakumar, E.; Senthilkumar, N.; Sureshkumar, K. Green synthesis of silver nanoparticles using *Piper longum* catkin extract irradiated by sunlight: antibacterial and catalytic activity. *Res. Chem. Intermed.* **2019**, *45*, 3617–3631.
- [55]. Alizadeh, S. R.; Seyedabadi, M.; Montazeri, M.; Khan, B. A.; Ebrahimzadeh, M. A. *Allium paradoxum* extract mediated green synthesis of SeNPs: Assessment of their anticancer, antioxidant, iron chelating activities, and antimicrobial activities against fungi, ATCC bacterial strains, *Leishmania* parasite, and catalytic reduction of methylene blue. *Mater. Chem. Phys.* **2023**, *296*, 127240.
- [56]. Singh, P.; Pandit, S.; Garnæs, J.; Tunjic, S.; Mokkaipati, V.; Sultan, A.; Thygesen, A.; Mackevica, A.; Mateiu, R. V.; Daugaard, A. E.; Baun, A.; Mijakovic, I. Green synthesis of gold and silver nanoparticles from *Cannabis sativa* (industrial hemp) and their capacity for biofilm inhibition. *Int. J. Nanomedicine* **2018**, *13*, 3571–3591.
- [57]. Hashemi, Z.; Shirzadi-Ahodashi, M.; Mortazavi-Derazkola, S.; Ebrahimzadeh, M. A. Sustainable biosynthesis of metallic silver nanoparticles using barberry phenolic extract: Optimization and evaluation of photocatalytic, in vitro cytotoxicity, and antibacterial activities against multidrug-resistant bacteria. *Inorg. Chem. Commun.* **2022**, *139*, 109320.
- [58]. Ebrahimzadeh, M. A.; Hashemi, Z.; Mohammadyan, M.; Fakhar, M.; Mortazavi-Derazkola, S. In vitro cytotoxicity against human cancer cell lines (MCF-7 and AGS), antileishmanial and antibacterial activities of green synthesized silver nanoparticles using *Scrophularia striata* extract. *Surf. Interfaces* **2021**, *23*, 100963.
- [59]. Alizadeh, S. R.; Biparva, P.; Goli, H. R.; Khan, B. A.; Ebrahimzadeh, M. A. Green synthesis of AuNPs by *Crocus caspius*—investigation of catalytic degradation of organic pollutants, their cytotoxicity, and antimicrobial activity. *Catalysts* **2022**, *13*, 63.
- [60]. Hashemi, Z.; Shirzadi-Ahodashi, M.; Ebrahimzadeh, M. A. Anti-leishmanial and antibacterial activities of biologically synthesized silver nanoparticles using *Alcea rosea* extract (AR-AgNPs). *J. Water Environ. Nanotechnol.* **2021**, *6*, 265–276.



Copyright © 2023 by Authors. This work is published and licensed by Atlanta Publishing House LLC, Atlanta, GA, USA. The full terms of this license are available at <http://www.eurjchem.com/index.php/eurjchem/pages/view/terms> and incorporate the Creative Commons Attribution-Non Commercial (CC BY NC) (International, v4.0) License (<http://creativecommons.org/licenses/by-nc/4.0>). By accessing the work, you hereby accept the Terms. This is an open access article distributed under the terms and conditions of the CC BY NC License, which permits unrestricted non-commercial use, distribution, and reproduction in any medium, provided the original work is properly cited without any further permission from Atlanta Publishing House LLC (European Journal of Chemistry). No use, distribution, or reproduction is permitted which does not comply with these terms. Permissions for commercial use of this work beyond the scope of the License (<http://www.eurjchem.com/index.php/eurjchem/pages/view/terms>) are administered by Atlanta Publishing House LLC (European Journal of Chemistry).